A Deep Learning-Based Approach to Power Minimization in Multi-Carrier NOMA with SWIPT

DOI:
10.1109/access.2019.2895201

Document Version
Accepted author manuscript

A Deep Learning-Based Approach to Power Minimization in Multi-Carrier NOMA with SWIPT

Jingci Luo, Jie Tang, *Senior Member*, *IEEE*, Daniel So, *Senior Member*, *IEEE*, Gaojie Chen *Senior Member*, *IEEE*, Kanapathippillai Cumanan, *Senior Member*, *IEEE*, and Jonathon Chambers, *Fellow*, *IEEE*

***Abstract*—Simultaneous wireless information and power transfer (SWIPT) and multi-carrier non-orthogonal multiple access (MC-NOMA) are promising technologies for future fifth generation (5G) and beyond wireless networks due to their potential capabilities in energy-efficient and spectrum-efficient system designs, respectively. In this paper, the joint downlink resource allocation problem for a SWIPT-enabled MC-NOMA system with time switching (TS)-based receivers is investigated, where pattern division multiple access (PDMA) technique is employed. We focus on minimizing the total transmit power of the system whilst satisfying the quality-of-service (QoS) requirements of each user in terms of data rate and harvested power. The corresponding optimization problem is a non-convex and a mixed integer programming problem which is difficult to solve. Different from the conventional iterative searching-based algorithms, we propose an efficient deep learning-based approach to determine an approximated optimal solution. Specifically, we employ a typical class of deep learning model, namely deep belief network (DBN), where the detailed procedure of the developed approach consists of three parts, i.e., data preparation, training and running. Simulation results demonstrate that the proposed DBN-based approach can achieve a similar performance of power consumption to the exhaustive search method. Furthermore, the results also confirm that MC-NOMA with PDMA outperforms MC-NOMA with sparse code multiple access (SCMA), single-carrier non-orthogonal multiple access (SC-NOMA) and orthogonal frequency division multiple access (OFDMA) in terms of power consumption in SWIPT-enabled systems.**

***Index Terms*—Non-orthogonal multiple access (NOMA), simultaneous wireless information and power transfer (SWIPT), machine learning.**

I. Introduction

With the dramatically rapid development of mobile Internet and the exponential growth of connected devices, the future wireless networks are expected to provide much higher data rate which enables supporting the proliferation of the Internet of things (IoT), massive machine-type communications (mMTC), etc [1]. However, the available radio spectrum is far from sufficient to support the unexpected high demands for data services, and hence it is particularly important to improve spectrum efficiency (SE) in the spectrum-limited systems. The conventional orthogonal multiple access (OMA) schemes, including orthogonal frequency-division multiple access (OFDMA) which is widely used in the fourth generation (4G) cellular systems, are increasingly arduous to fulfill the aforementioned unprecedented requirements due to the limited improvement of SE in orthogonal channel access [2]. The non-orthogonal multiple access (NOMA) technique, which allows multiple users to share the same time-frequency resource element (RE), has been recognized as the potential multiple access technique to achieve higher SE in future fifth generation (5G) and beyond wireless networks [3]. Furthermore, heterogeneous requirements such as ultra-low latency, ultra-reliability and massive connectivity are more likely to be realized in NOMA systems.

Since the system-level performance of NOMA has been proved to be superior to OMA under various wireless environments in [4]–[6], NOMA has attracted a significant attention in both academia and industry. Several forms of NOMA techniques have been proposed for 5G and beyond wireless networks. Depending on whether the total available spectrum resource is or is not divided into several subcarriers, NOMA can be classified into two main types, namely single-carrier NOMA (SC-NOMA) and multi-carrier NOMA (MC-NOMA), respectively. The power-domain NOMA (PD-NOMA) is a well-known and promising SC-NOMA technique [7], in which multiple users are multiplexed with different transmit power levels in the same frequency RE and successive interference cancelation (SIC) is employed at the receiver ends to remove the corresponding co-channel interference so that better performance in terms of SE, energy efficiency (EE) or proportional fairness can be achieved [8], [9]. On the other hand, sparse code multiple access (SCMA) [10] and pattern division multiple access (PDMA) [11] are two most well-known techniques of MC-NOMA. In fact, these two MC-NOMA techniques can be considered as the superposition of multiple PD-NOMAs in different frequency REs [12].

In addition to the efficient spectrum utilization, energy saving is another key issue in future green communication, as the contradiction between the tremendous energy consumption

This work has been supported in part by the National Natural Science Foundation of China under Grant 61601186, in part by the Natural Science Foundation of Guangdong Province (2017A030313383), and in part by the open research fund of National Mobile Communications Research Laboratory, Southeast University (No. 2019D06). *(Corresponding author: Jie Tang.)*

J. Luo is with the School of Electronic and Information Engineering, South China University of Technology, Guangzhou, China. (e-mail: 201720110615@mail.scut.edu.cn).

J. Tang is with the School of Electronic and Information Engineering, South China University of Technology, Guangzhou, China, and also with National Mobile Communications Research Laboratory, Southeast University, Nanjing 210096, China (e-mail: eejtang@scut.edu.cn).

D. K. C. So is with the School of Electrical and Electronic Engineering, University of Manchester, Manchester, United Kingdom. (e-mail: d.so@manchester.ac.uk).

K. Cumanan is with the Department of Electronic Engineering, University of York, United Kingdom. (e-mail: kanapathippillai.cumanan@york.ac.uk).

G. Chen and J. A. Chambers are with the Department of Engineering, University of Leicester, United Kingdom. (email: gaojie.chen@leicester.ac.uk; jonathon.chambers@leicester.ac.uk).

caused by wireless communication systems and the global energy shortage is intensifying. Thus, it is crucial to improve EE in future wireless networks for their sustainability. Motivated by the progress in the research on wireless power transfer (WPT) [13] and the fact that the radio frequency (RF) signal is the carrier of both information and energy, an advanced technology namely simultaneous wireless information and power transfer (SWIPT) has been identified to meet the demanding requirements in future wireless networks in [14]. In order to deal with the sensitivity difference between the information receiver and the energy receiver, two practical receiver architecture designs namely time switching (TS) and power splitting (PS) have been developed in [15] where information decoding (ID) and energy harvesting (EH) could be separated through time domain and power domain, respectively. The purpose of SWIPT is to reduce energy waste and prolong the battery-life of communication terminals by simultaneously harvesting energy and receiving information. Furthermore, SWIPT is viewed as a potential energy-efficient solution for 5G and beyond wireless networks [13] and a great deal of research has been carried out on the application of SWIPT technology in different systems, including OFDMA systems [16], multiple-input single-output (MISO) systems [17], [18], multiple-input multiple-output (MIMO) systems [19], heterogenous cellular networks [20] and two way cooperative networks [21], etc.

A. Related works

In the literature, many works have explored the combination of SWIPT technology and NOMA network to reduce the power consumption of the terminals. For instance, studies on SWIPT-based SC-NOMA systems have been investigated in [22]–[26]. Specifically, the work in [22] considered incorporating the SWIPT in cooperative MISO SC-NOMA systems and developed a strategy of jointly optimizing PS ratio and the beamforming vectors to maximize the data rate of the "strong user" while satisfying the QoS requirements of "weaker user". In [26], sum secrecy rate (SSR) maximization problem was addressed in a SWIPT-based SC-NOMA system, and the numerical results demonstrated that the performance gains in terms of SSR could be achieved over the conventional OMA as well as the SWIPT-based OMA systems.

Additionally, Zhai *et al.* have combined the SWIPT with MC-NOMA in [27] by employing SCMA technique where an optimization framework was developed to strike a good balance between the conflicting performance metrics, namely, data rate and harvested energy. Nevertheless, the performance of the combination of the SWIPT and the MC-NOMA with PDMA remains unknown. Since Zeng *et al.* have confirmed that PDMA outperforms SCMA in terms of both system throughput performance and block error ratio (BLER) performance [28], it is worth studying on SWIPT-aided MC-NOMA systems with PDMA technique.

B. Contributions

In this paper, we solve a power minimization problem in the downlink of SWIPT-enabled and PDMA-based MC-NOMA system with TS-based receivers. In particular, we aim to develop a joint optimal solution of subscarrier assignment, power allocation as well as the TS ratio. In general, this kind of joint resource allocation problems are non-deterministic polynomial (NP) hard, and thus the corresponding optimal solutions are of great computational complexity with conventional approaches. Recently, deep learning methods have been exploited to solve the fundamental high complex resource allocation problems in wireless communication systems. More specifically, deep learning methods were developed for solving the problem of route estimation in [29], network traffic classification in [30], mobility prediction [31], resource allocation [32], etc. Motivated by the aforementioned works, we exploit deep learning technique to determine an approximated optimal joint resource allocation strategy for the complicated optimization problem in the considered system.

The main contributions in this work are summarized in the following:

- A deep learning-based resource allocation framework is developed to solve the high complex power minimization problem, which consists of three parts:
  1) *Data preparation:* we randomly generate a set of channel gains, i.e., the input of the training sample; and then we apply the well-known genetic algorithm to determine the corresponding optimal solution, i.e., the output of the training sample.
  2) *Training:* we establish a deep belief network (DBN) for each parameter to be optimized, and train the DBNs based on the obtained samples through both unsupervised and supervised trainings.
  3) *Running:* with a given input (channel gains), the well-trained DBNs are exploited to directly approximate the optimal solution of the considered power minimization problem.
- Numerical results demonstrate that the developed deep learning-based approach can achieve a similar performance of power consumption to the exhaustive search method as well as the genetic algorithm.
- It is also proven that the performance of the proposed MC-NOMA with PDMA is superior to that of the existing MC-NOMA with SCMA, SC-NOMA and OFDMA in SWIPT-enabled systems in terms of power saving.

The remainder of this paper is organized as follows. In Section II, we present the system model of the considered SWIPT-enabled MC-NOMA system with PDMA and mathematically formulate the total transmit power minimization problem. The proposed deep learning-based resource allocation framework is defined and developed in Section III. In Section IV, we evaluate the performance of our proposed algorithm through numerical simulations. Finally, the conclusions of this work are provided in Section V.

The following notations are used throughout the paper. We use the lower-case boldface letters for vectors and uppercase boldface letters for matrices. $\mathbb{N}$ denotes the natural number set while $\mathbb{R}_+$ denotes the non-negative real number set. $\mathbb{E}[|x|^2]$ represents the energy of signal x and $\mathbf{x}'$ indicates the transposition of $\mathbf{x}$.

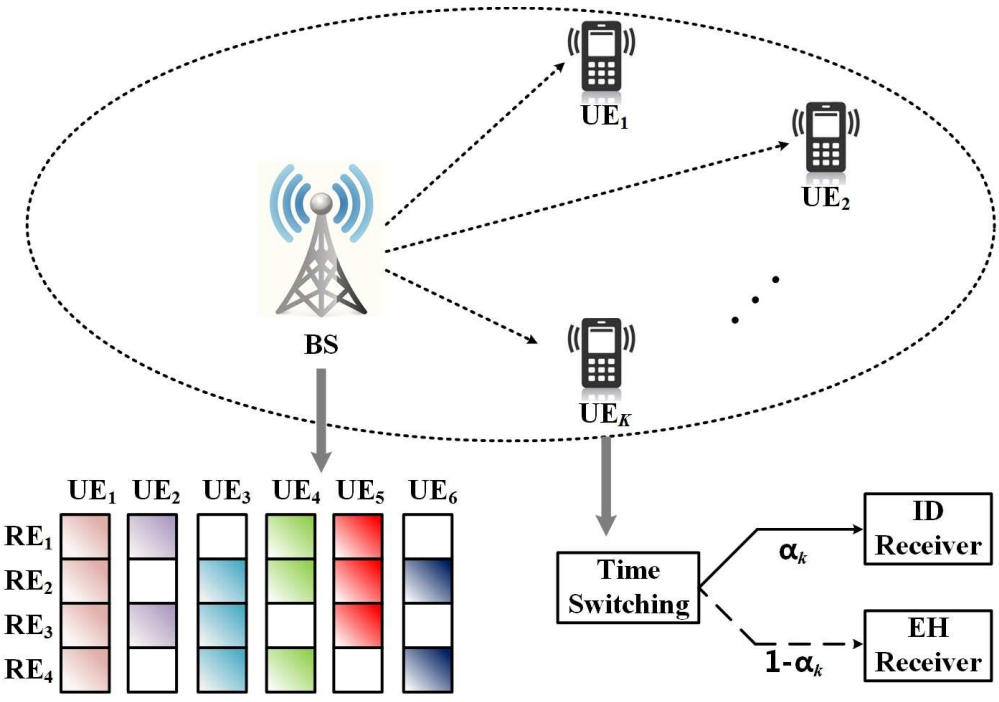

Fig. 1: The system model of a downlink SWIPT-enabled MC-NOMA with TS-based receivers and PDMA technique.

II. System Model and Problem Formulation

In this section, we first present the system model of the downlink of SWIPT-enabled MC-NOMA with TS-based receivers and PDMA technique. Then the total transmit power minimization problem is mathematically formulated.

A. System Model

As shown in Fig. 1, the considered downlink SWIPT-enabled MC-NOMA system consists of a base station (BS) and K users superposed on N subcarriers through PDMA technique. It is assumed that the transmitter and all the receivers are equipped with one single antenna. Let us denote the set of all users' indexes by $\mathcal{K} \triangleq \{1, 2, \ldots, K\}$ while the set of all subcarriers' indexes by $\mathcal{N} \triangleq \{1, 2, \ldots, N\}$. The total bandwidth B is equally divided into N subcarriers and thus the bandwidth of each subchannel is denoted as $B_c = B/N$. It is assumed that there is no interference between different subchannels due to the orthogonal frequency division. Note that PDMA is based on SIC amenable multiple access (SAMA) technique which can be completed in different domains such as code domain, power domain, space domain or their combinations. In particular, the design of PDMA includes unequal diversity at the transmitter side and equal diversity at the receiver side. For convenience, the mapping of transmitted signal to a group of subcarriers can be described as a $N \times K$ characteristic pattern matrix $\mathbf{Q_{PDMA}} \in \mathbb{N}^{N \times K}$. The element in the nth row and the kth column of $\mathbf{Q_{PDMA}}$ $q_{n,k} = 1$ indicates the signal transmitted to the kth user (UE$_k$) is superposed on the nth subcarrier (RE$_n$) while $q_{n,k} = 0$ indicates the opposite. Let $\mathcal{N}_n = \{k | q_{n,k} = 1\} (n \in \mathcal{N})$ and $|\mathcal{N}_n| = \sum_{k=1}^{K} q_{n,k} (n \in \mathcal{N})$ respectively denote the set and the number of UEs mapped on RE$_n$.

For example, the corresponding characteristic pattern matrix of the mapping schematic diagram in Fig. 1 can be given as

$$\mathbf{Q_{PDMA}}^{(4,6)} = \begin{pmatrix} 1 & 1 & 0 & 1 & 1 & 0 \\ 1 & 0 & 1 & 1 & 1 & 1 \\ 1 & 1 & 1 & 0 & 1 & 0 \\ 1 & 0 & 1 & 1 & 0 & 1 \end{pmatrix}, \tag{1}$$

where the signal of the UE$_1$ is mapped to all four REs; the signal of the UE$_2$ is superposed in the RE$_1$ and RE$_3$; etc. The number of transmission diversity of these six UEs is 4, 2, 3, 3, 3 and 2, respectively. Moreover, $\mathcal{N}_1 = \{1, 2, 4, 5\}$ and $|\mathcal{N}_1| = 4$, etc.

We denote the transmit power allocated to the UE$_k$ on RE$_n$ as $P_{n,k}$. Hence, the received signal of UE$_k$ via RE$_n$ can be expressed as

$$y_{n,k} = h_{n,k} \left(q_{n,k} \sqrt{P_{n,k}} x_{n,k} + \sum_{\substack{j \in \mathcal{K}, \\ j \neq k}} q_{n,j} \sqrt{P_{n,j}} x_{n,j} \right) + z_{n,k}, \tag{2}$$

where $h_{n,k} = g_{n,k} d_k^{-\beta}$ denotes the channel coefficient from the BS to UE$_k$ via RE$_n$; $g_{n,k}$ represents the small-scale fading and follows a Rayleigh distribution with unit variance. The $d_k^{-\beta}$ denotes the large-scale fading; d_k is the distance between the BS and UE$_k$ while β is the related path-loss exponent; $x_{n,k}$ ($x_{n,j}$) is the data symbol transmitted from the BS to UE$_k$ (UR$_j$) via subcarrier RE$_n$ with unit energy $\mathbb{E}[|x_{n,k}|^2]$ ($\mathbb{E}[|x_{n,j}|^2]$); and $z_{n,k} \sim \mathcal{CN}(0, \sigma_n^2)$ is the additive white Gaussian noise (AWGN) on RE$_n$. For notation simplicity, we normalize the channel coefficient as $\widetilde{h}_{n,k} = |h_{n,k}|^2 / \sigma_n^2$, which is redefined as the channel to noise ratio (CNR).

Since the subcarrier sharing will inevitably cause intra-band interference, SIC technology is employed at the receiver side to mitigate the interference and improve the decoding performance. Let $\boldsymbol{\pi}(n) \triangleq (\pi_n(1), \pi_n(2), \ldots, \pi_n(|\mathcal{N}_n|))$ denote the decoding order of the UEs on RE_n, which can be viewed as a vector function of the CNR of each UE mapped on RE_n, i.e., $\widetilde{h}_{n,k}$ ($k \in \mathcal{N}_n$). In particular, in the downlink of NOMA, the cancellation order at every UE is always to decode the UEs with weaker CNR and subtract the signals of these UEs firstly, and then decode its own data by treating the signals of the remaining UEs on RE_n as interference [33]. Hence, we have $\widetilde{h}_{n,\pi(1)} < \widetilde{h}_{n,\pi(2)} < \ldots < \widetilde{h}_{n,\pi(|\mathcal{N}_n|)}$. Based on SIC technique and with this decoding order, the normalized interference for UE_k on RE_n is hence given by

$$I_{n,k} = \widetilde{h}_{n,k} \sum_{\substack{j \in \mathcal{N}_n, \\ \widetilde{h}_{n,j} > \widetilde{h}_{n,k}}} q_{n,j} P_{n,j}. \tag{3}$$

Accordingly, the signal to interference-plus-noise ratio (SINR) of UE_k on RE_n can be written as

$$\gamma_{n,k} = \frac{\widetilde{h}_{n,k} q_{n,k} P_{n,k}}{1 + I_{n,k}}. \tag{4}$$

In practice, the outage may occur if the SINR does not meet the minimum SINR requirement $\overline{\gamma}$, which will lead to the failure of SIC process. In order to avoid this outage, we must have the following condition:

$$\gamma_{n,k} \geq \overline{\gamma}, \quad \forall n \in \mathcal{N}, \quad \forall k \in \mathcal{N}_n. \tag{5}$$

With this condition, the available data rate of UE_k on RE_n can be written as

$$R_{n,k} = B_c \log_2(1 + \gamma_{n,k}). \tag{6}$$

Furthermore, we consider SWIPT-enabled UE in our proposed system model, which consists of an ID circuit and an EH rectification circuit. TS scheme is employed to achieve ID and EH in two orthogonal time slots. For UE_k, α_k and $1-\alpha_k$ correspond to the portion of transmission time allocated to ID and EH, respectively. Hence, the data rate of UE_k based on TS scenario can be denoted as

$$R_k^{TS} = \alpha_k \sum_{n \in \mathcal{N}} R_{n,k}. \tag{7}$$

On the other hand, the power that can be harvested by UE_k via RE_n is given by

$$E_{n,k} = \eta |h_{n,k}|^2 \sum_{j \in \mathcal{K}} q_{n,j} P_{n,j}, \tag{8}$$

where η denotes the power conversion efficiency of the EH rectification circuits.

Therefore, the power harvested by UE_k based on TS scheme can be expressed as

$$E_k^{TS} = (1 - \alpha_k) \sum_{n \in \mathcal{N}} E_{n,k}. \tag{9}$$

B. Problem Statement

From energy-efficient communication systems perspective, we formulate a total transmit power minimization problem with the QoS requirements and transmit power constrains for the system defined in the previous subsection. In particular, the total transmit power is given as

$$P_{total} = \sum_{n=1}^{N} \sum_{k=1}^{K} q_{n,k} P_{n,k}. \tag{10}$$

The transmit power minimization problem can be mathematically formulated as follows:

$$\begin{aligned}
\text{P1}: \quad & \min_{\boldsymbol{\alpha}, \mathbf{Q}, \mathbf{P}} \quad P_{total} && (11)\\
& \text{s.t.} \quad (5), && (12)\\
& \quad R_k^{TS} \geq R_{req}, \quad \forall k \in \mathcal{K}, && (13)\\
& \quad E_k^{TS} \geq E_{req}, \quad \forall k \in \mathcal{K}, && (14)\\
& \quad 0 < \alpha_k < 1, \quad \forall k \in \mathcal{K}, && (15)\\
& \quad q_{n,k} \in \{0, 1\}, \quad \forall n \in \mathcal{N}, \quad \forall k \in \mathcal{K}, && (16)\\
& \quad 0 \leq P_{n,k} \leq \overline{P}, \quad \forall n \in \mathcal{N}, \quad \forall k \in \mathcal{K}, && (17)
\end{aligned}$$

where $\boldsymbol{\alpha} = [\alpha_1, \alpha_2, \ldots, \alpha_K]^T$ is the vector that consists of TS ratios of the all UEs, $\mathbf{Q} \in \mathbb{N}^{N \times K}$ denotes the PDMA characteristic pattern matrix and $\mathbf{P} \in \mathbb{R}_+^{N \times K}$ represents the power allocation matrix. The constraints provided in (12) define the minimum SINR requirements that ensure a successful implementation of the SIC technique. The inequalities in (13) and (14) are associated with the constraints of QoS requirements, including data rate and harvested power. In addition, R_{req} and E_{req} denote the minimum data rate and harvested power requirements at each UE, respectively. The constraints in (15) indicate that the TS ratio for each UE is required to be in the range of $(0, 1)$. In (16), every element of the PDMA pattern matrix $q_{n,k} (n \in \mathcal{N}, k \in \mathcal{K})$ can only be either 0 or 1, indicating whether or not UE_k is mapped on RE_n. Besides, the transmit power allocated to UE_k on RE_n should meet the constraint $0 \leq P_{n,k} \leq \overline{P}$, where $\overline{P}$ is the transmit power limitation which ensures maintaining a fairness among UEs.

Note that the convexity of the objective function (11) cannot be established in general due to the binary variables $q_{n,k}$ as well as the product of $q_{n,k}$ and $P_{n,k}$ ($n \in \mathcal{N}, k \in \mathcal{K}$). Similarly, the convexity of the inequality constraints in (12)-(14) also does not exist. Consequently, the aforementioned power minimization problem P1 is a non-convex and a mixed integer programming problem. In addition, this is a well-known NP-hard problem [34], which makes it considerably strenuous to determine the joint optimal solution. In addition to the exhaustive searching method, there are many iterative algorithms available in the literature for seeking the optimal solution for non-convex programming, such as the genetic algorithm and the simulated annealing. Nevertheless, these algorithms always require a huge amount of time to converge, which are not suitable for real-time processing networks. To overcome these difficulties, we propose a deep learning-based approach in the following section to determine an approximated optimal solution for the problem P1.

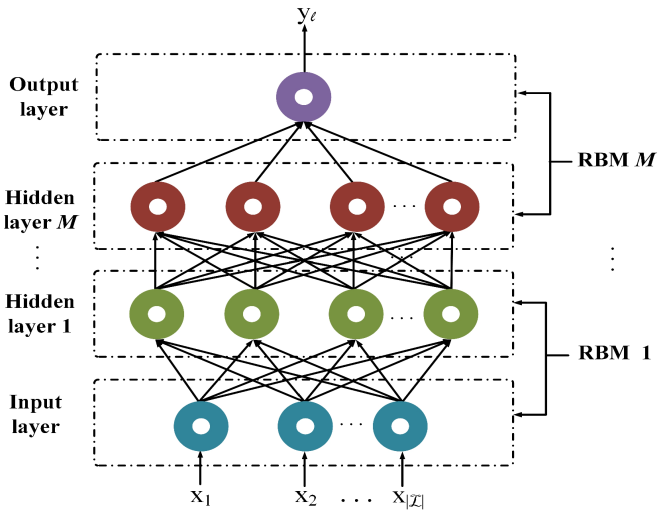

Fig. 2: An example of the DBN framework used in this work.

III. Total Power Minimization by Deep Learning

In this section, we firstly provide a brief description on the framework of the considered deep learning model, namely, DBN. Then, the detailed procedure of the proposed DBN-based approach is developed, which consists of three parts, i.e., data preparation, model training and solution running.

A. Framework of DBN

Prior to developing a specific procedure of the deep learning-based approach, we first briefly introduce the DBN. This model is a representive class of deep learning networks and is capable of capturing the potential information between the input and the output datas [35]. As shown in Fig. 2, the architecture design of the DBN involves an input layer, a set of hidden layers and an output layer, which can be also considered as a series of restricted Boltzmann machines (RBMs). Each RBM consists of a visible layer and a hidden layer. In particular, the neurons between the visible and the hidden layers are fully connected with a certain weight while those neurons within the same layer are disconnected. Furthermore, the first RBM takes the input layer of the DBN as its visible layer and the first hidden layer of the DBN as its own hidden layer; the second RBM takes the hidden layer of the previous RBM as its visible layer and the second hidden layer of the DBN as its own hidden layer; etc. The training procedure for each DBN includes two phases. In the first phase, the RBMs are trained one by one with unsupervised learning to roughly determine the parameters of the DBN. In the second phase, all the parameters of the DBN are fine-tuned with supervised learning according to the back-propagation algorithm. More details of training procedure of the DBNs are given in Section IV-C.

B. Data Preparation Part

To the best of our knowledge, deep learning technique can be considered as a comprehensive tool to derive knowledge from sufficient empirical data. Hence, a large number of data samples are required to develop a deep learning-based approach to approximate the optimal solution. In our work, we firstly randomly generate channel coefficients $h_{n,k}(n \in \mathcal{N}, k \in \mathcal{K})$ and then employ the genetic algorithm to deal with the optimization problem P1 to determine the optimal solution including the characteristic pattern matrix $\mathbf{Q}^*$, the power allocation $\mathbf{P}^*$ and the TS ratio control $\boldsymbol{\alpha}^*$. In our work, the input of the training sample $\mathbf{x}$ is composed of the channel coefficients while the output $\mathbf{y}$ is related to the optimal solution that determined by genetic algorithm, which can be more clearly expressed as

$$\mathbf{x} = [h_{1,1}, \ldots, h_{1,K}, \ldots, h_{N,1}, \ldots, h_{N,K}], \tag{18}$$

$$\begin{aligned}\mathbf{y} =& [q^*_{1,1}, \ldots, q^*_{1,K}, \ldots, q^*_{N,1}, \ldots, q^*_{N,K},\\ & P^*_{1,1}, \ldots, P^*_{1,K}, \ldots, P^*_{N,1}, \ldots, P^*_{N,K},\\ & \alpha^*_1, \ldots, \alpha^*_K].\end{aligned} \tag{19}$$

Note that there are K UEs communicating with the BS via N REs in the considered system, the vector $\mathbf{y}$ is consisted of $2NK + K$ elements and we need to approximate totally $2NK+K$ output parameters. Hence, we will establish $2NK+K$ DBNs for all parameters in the next part, which are denoted as DBN$_\ell$ ($\ell \in 1, 2, \ldots, 2NK + K$). In particular, the set of training samples for DBN$_\ell$ is given by $\{(\mathbf{x}, y_\ell)\}$, where y_ℓ is the ℓth component of $\mathbf{y}$ and $\ell \in \{1, 2, \ldots, 2NK + K\}$.

C. Model Training Part

With sufficient training samples obtained in the previous part, we now start training the DBN for each parameter to be estimated one by one. For each RBM in DBN$_\ell$, we denote $\mathbf{v}$ and $\mathbf{h}$ as the vector of the visible layer and the hidden layer, respectively.

The first stage of the training process is unsupervised learning. First of all, the corresponding parameters of the RBM are initialized, including the weights between the visible and hidden layers $\mathbf{w}$, the biases related to the visible layer $\mathbf{b}_v$ and the biases associated with the hidden layer $\mathbf{b}_h$. Let $\Phi = \{\mathbf{w}, \mathbf{b}_v, \mathbf{b}_h\}$. Next, these parameters are updated iteratively according to the following expression:

$$\Phi_{t+1} = \Phi_t + \varepsilon \frac{\partial \log Pr(\mathbf{v}_t)}{\partial \Phi_t}, \tag{20}$$

where t and ε denote the number of iteration and the learning rate in the unsupervised training stage, respectively. Furthermore, $Pr(\mathbf{v}_t)$ corresponds to the probability of the visible layer in the tth iteration $\mathbf{v}_t$, which can be calculated through the joint probability distribution of the visible and the hidden layers $Pr(\mathbf{v}_t, \mathbf{h}_t)$. Hence, $Pr(\mathbf{v}_t)$ can be defined as

$$\begin{aligned} Pr(\mathbf{v}_t) &= \sum_{\mathbf{h}_t} Pr(\mathbf{v}_t, \mathbf{h}_t)\\ &= \sum_{\mathbf{h}_t} \frac{\exp\left(-E\left(\mathbf{v}_t, \mathbf{h}_t\right)\right)}{\sum_{\mathbf{v}_t}\sum_{\mathbf{h}_t} \exp\left(-E\left(\mathbf{v}_t, \mathbf{h}_t\right)\right)}. \end{aligned} \tag{21}$$

In (21), $E(\mathbf{v}_t, \mathbf{h}_t)$ is the energy function related to the RBM, which can be calculated by

$$E(\mathbf{v}_t, \mathbf{h}_t) = -\mathbf{v}'_t \mathbf{w}_t \mathbf{h}_t - \mathbf{b}'_{v_t} \mathbf{v}_t - \mathbf{b}'_{h_t} \mathbf{h}_t. \tag{22}$$

It should be noted that it takes considerably long time to calculate the joint probability distribution $Pr(\mathbf{v}_t, \mathbf{h}_t)$ according to (21) and (22) due to the high computational complexity. For convenience, an approximate of $Pr(\mathbf{v}_t, \mathbf{h}_t)$ based on Gibbs sampling has been exploited to tackle this complexity issue in our work.

The second stage of training process is supervised learning. The purpose of this stage is to fine-tune the parameters of DBN_ℓ based on the output of the training sample, i.e., y_ℓ. Denote $y_\ell^{(i)}$ as the output of the ith training sample and the $\widehat{y}_\ell^{(i)}$ as the output predicted by the DBN_ℓ with the given input $\mathbf{x}^{(i)}$. The process of fine-tuning can be mathematically formulated as minimizing a loss function namely cross entropy, which is given as

$$\mathcal{S}_\ell = -\frac{1}{D}\sum_{i=1}^{D}\left(y_\ell^{(i)}\log(\widehat{y}_\ell^{(i)}) + (1-y_\ell^{(i)})\log(1-\widehat{y}_\ell^{(i)})\right), \tag{23}$$

where D is the number of the training samples. In fact, the cross entropy $\mathcal{S}_\ell$ is the measure of prediction error of DBN_ℓ. At the end, the set of parameters Φ is fine-tuned iteratively by the back-propagation algorithm, which can be expressed as follow:

$$\Phi_{t+1} = \Phi_t - \widetilde{\varepsilon}\frac{\partial \mathcal{S}}{\partial \Phi_t}, \tag{24}$$

where $\widetilde{\varepsilon}$ corresponds to the learning rate of the back-propagation algorithm in the supervised training stage.

D. Solution Running Part

In the solution running part, we first randomly generate the channel gains $h_{n,k}(n \in \mathcal{N}, k \in \mathcal{K})$, and the input layer of DBN is denoted as $\mathbf{x} = [h_{1,1}, \ldots, h_{1,K}, \ldots, h_{N,1}, \ldots, h_{N,K}]$. Then the well-trained DBN networks (DBN_1, DBN_2, …, DBN_{2NK+K}) are loaded. With the given input $\mathbf{x}$ and the well-trained DBN_ℓ, we can compute and predict the output layer of each DBN_ℓ, denoting as $\widehat{y}_\ell$. Finally, we form the approximate of the optimal solution (including $\widehat{\mathbf{Q}}$, $\widehat{\mathbf{P}}$ and $\widehat{\boldsymbol{\alpha}}$) of the power minimization problem P1 based on the output of each DBN, i.e.,

$$\widehat{\mathbf{Q}} = \begin{pmatrix} \widehat{y}_1 & \cdots & \widehat{y}_K \\ \vdots & \ddots & \vdots \\ \widehat{y}_{(N-1)K+1} & \cdots & \widehat{y}_{NK} \end{pmatrix}, \tag{25}$$

$$\widehat{\mathbf{P}} = \begin{pmatrix} \widehat{y}_{NK+1} & \cdots & \widehat{y}_{NK+K} \\ \vdots & \ddots & \vdots \\ \widehat{y}_{(2N-1)K+1} & \cdots & \widehat{y}_{2NK} \end{pmatrix}, \tag{26}$$

and

$$\widehat{\boldsymbol{\alpha}} = [\widehat{y}_{2NK+1}, \ldots, \widehat{y}_{2NK+K}]. \tag{27}$$

Up to now, the complete procedure of the proposed DBN-based approach to approximate the optimal solution of the formulated transmit power minimization problem is summarized in TABLE I.

INPUT:
The randomly generated channel gains between BS and UE_k on RE_n, $h_{n,k}(n \in \mathcal{N}, k \in \mathcal{K})$;
OUTPUT:
The approximation of the optimal solution of resource allocation, including the characteristic pattern $\widehat{\mathbf{Q}}$, the power allocation $\widehat{\mathbf{P}}$ and the TS ratio control $\widehat{\boldsymbol{\alpha}}$;
Generate sufficient training samples $\{(\mathbf{x}, \mathbf{y})\}$:
$\mathbf{x}$ corresponds to the randomly generated channel gains while $\mathbf{y}$ corresponds to the optimal solution determined by genetic algorithm; the details are given in (18) and (19), respectively.
Train the framework of DBNs one by one:
set the stopping criteria ϵ_1 and ϵ_2;
for $\ell = 1 : 2NK + K$
  for $m = 1 : M$
    initialize the parameters vector Φ of the mth RBM;
    Unsupervised learning stage:
    repeat
      update the parameters vector Φ according to (20);
    until $\|\Phi_{t+1} - \Phi_t\| \le \epsilon_1$;
    Supervised learning stage:
    repeat
      fine-tune the parameters Φ by back-propagation algorithm according to (24);
    until $\|\Phi_{t+1} - \Phi_t\| \le \epsilon_2$;
  end
end
Predict the optimal resource allocation solution:
for $\ell = 1 : 2NK + K$
  load the well-trained framework of DBN_ℓ; compute $\widehat{y}_\ell$ through DBN_ℓ with the given channel gains;
end
form the approximation of the optimal solution according to (25), (26) and (27);
RETURN: $\widehat{\mathbf{Q}}$, $\widehat{\mathbf{P}}$ and $\widehat{\boldsymbol{\alpha}}$;

TABLE I: The complete procedure of the proposed DBN-based approach for total transmit power minimization

IV. Simulation Results

In this section, numerical results are provided to evaluate the performance of our proposed deep learning-based joint resource allocation approach for minimizing the total transmit power. It is assumed that the BS is located in the center of the cellular network and all UEs are randomly distributed within a circle with radius of 300 meters. In other words, the distance between BS and the kth UE d_k is randomly generated within the range $(0, 300)$. The system bandwidth is assumed to be $B = 4$ MHz. Referring to the typical 3GPP propagation environment in [36], we set the path-loss exponent $\beta = 3.76$. The detailed radio propagation model has been discussed in Section II-A and it is omitted here for brevity. Furthermore, the power conversation efficiency of the EH circuits is set to be $\eta = 30\%$; the minimum data rate requirement and harvested power for each UE are assumed to be $R_{req} = 1$ Mbit/s and $E_{req} = 0.1$ W, respectively. Other system parameters are

provided with the corresponding simulation results. In order to construct, train and run the DBNs in our proposed approach, the well-known and powerful off-the-shelf programming tool namely *Tensorflow r1.8* is used by implementing in the *Python 3.6.0* platform.

First, we study the effectiveness of the proposed deep learning-based approach by comparing the predicted result with that obtained by exhaustive search method as well as genetic algorithm. For this study, we consider an example of a system with 4 UEs and 2 REs. The maximum available transmit power is set to be $\overline{P} = 1$ W and the noise power on the nth subchannel is assumed to be $\sigma_n^2 = 0.01$ W $(n = \{1, 2\})$. To the beginning, we randomly generate the channel gains and determine the input of the sample $\mathbf{x}$ based on (18); then solve the problem P1 through genetic algorithm to establish the output of the sample $\mathbf{y}$ according to (19). This process is repeated for 10000 times to generate 10000 training samples $\{(\mathbf{x}, \mathbf{y})\}$. Next, these 10000 samples are used to trained the DBNs. Each DBN$_\ell$ consists of five layers, including an input layer $\mathbf{x}$, three hidden layers and an output layer y_ℓ. The number of neurons in each layer is set to be 8, 64, 128, 128 and 1, respectively. In addition, the learning rates are respectively set to be $\varepsilon = 0.0001$ and $\widetilde{\varepsilon} = 0.0001$; the number of training epochs is set to be 3000; and the terminating thresholds are set to be $\epsilon_1 = 1e^{-3}$ and $\epsilon_2 = 1e^{-3}$, respectively. In the solution running part, we approximate the optimal solution by the well-trained DBNs and the corresponding performance is compared to that of the exhaustive search method and the genetic algorithm. As shown in Fig. 3, the performance obtained by the genetic algorithm is very similar to the one derived by the exhaustive search method. However, it takes about 800 iterations to converge, which requiers a lot of time. In particular, it takes much longer time for the genetic algorithm to converge as the number of UEs and REs increases, and thus it fails to meet the fundamental requirements of ultra-low latency in the communication networks. On the other hand, it can be seen in Fig. 3 that the performance gap between the proposed DBN-based approach and the exhaustive search method is small which is acceptable to some extent. More importantly, it takes less time to approximate the optimal solution through the proposed DBN-based approach, which facilitates to meet the stringent requirement of ultra-low latency.

Next, the performance in terms of the minimum required total transmit power under various system parameters is evaluated in Fig. 4. It should be noted that all the simulation results are based on the architecture design of DBNs discussed in the previous simulation, and each result under a certain setting of system parameters is the average of the approximations corresponding to 1000 groups of randomly generated channels. In particular, we assume that the total bandwidth is divided into 4 subcarriers, i.e., $N = 4$ and $B_c = 1$ MHz. The noise power in any subcarrier is set to be $\sigma_n^2 = 0.001/0.01/0.1$ W for comparison. As shown in Fig. 4, under the same setting of noise power, the minimum total transmit power approximated by deep learning-based approach is monotonically increasing with the increase in the number of UEs. Furthermore, the transmit power consumption always increases with the increase in

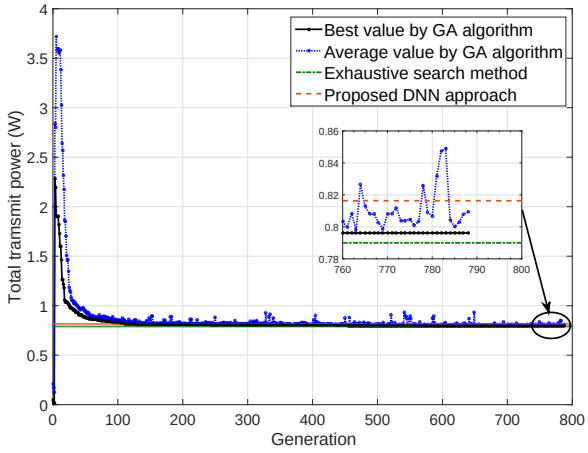

Fig. 3: Performance evaluation of genetic algorithm and the proposed DBN-based approach

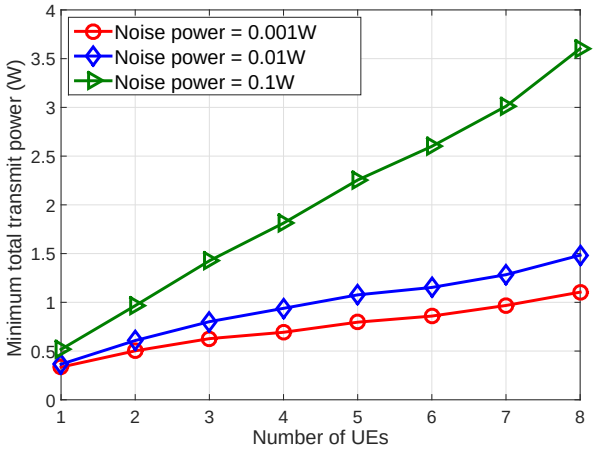

Fig. 4: Comparison of minimum total transmit power of the proposed approach against different number of UEs with different noise power

the noise power, regardless of the number of UEs. In particular, the relationship between the minimum transmit power and the number of UEs can be approximated as a linear function and the slope of it will increase with the increase in the noise power.

Next, we study the minimum total transmit power estimated by the proposed deep learning-based strategy with different levels of QoS requirements. The minimum data rate requirement per user is set to vary from 0.2 Mbit/s to 2 Mbit/s while the minimum demand of harvested power is set to vary from 0.02 W to 0.2 W. Furthermore, the number of subcarriers and the noise power are assumed to be $N = 4$ and $\sigma_n^2 = 0.01$ W, respectively. The number of UEs is assumed to be $3/4/5$ for comparison. As shown in Fig. 5, the increasing level of minimum data rate requirement leads to an increasing total transmit power and this tendency becomes more and more obvious as the number of UEs increases. Similar result can be observed in Fig. 6 where the total transmit power monotonically increases with the increase in the level of minimum requirement of harvested power. These

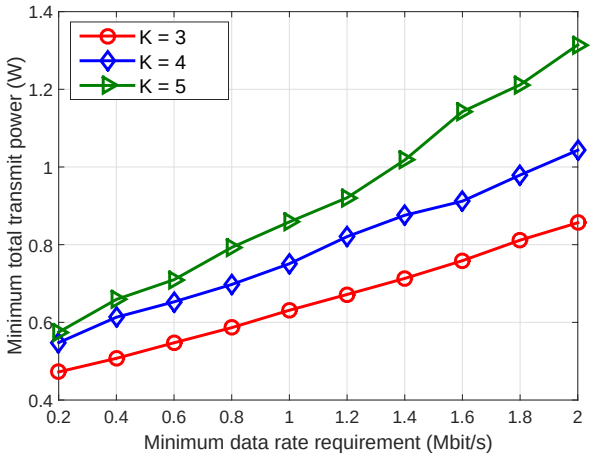

Fig. 5: Comparison of minimum total transmit power of the proposed approach with different minimum data rate requirements

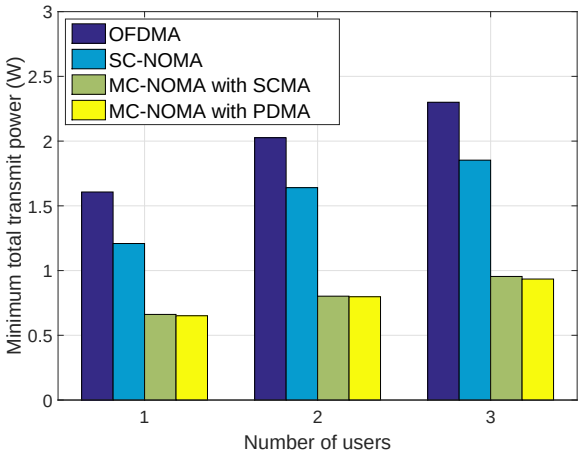

Fig. 7: Comparison of minimum total transmit power among OFDMA, SC-NOMA, MC-NOMA with SCMA and MC-NOMA with PDMA in SWIPT-enabled systems

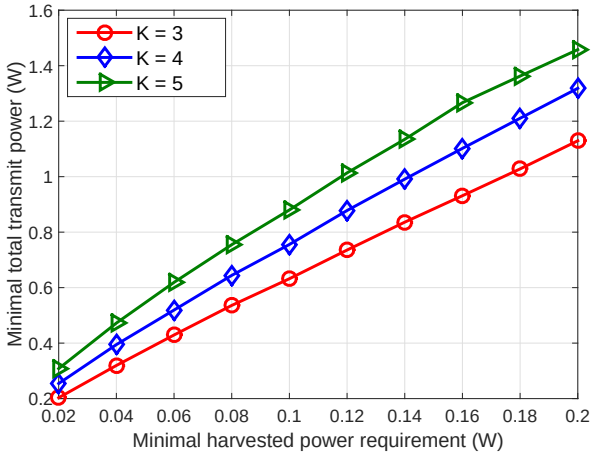

Fig. 6: Comparison of minimum total transmit power of the proposed approach with different minimum harvested power requirements

results confirm and validate the effectiveness of the proposed deep learning-based approach.

Finally, we study the performance comparison in terms of transmit power minimization between the MC-NOMA with PDMA scheme and the OFDMA, SC-NOMA or MC-NOMA with SCMA scheme in SWIPT-enabled systems. The number of UEs is set to be $3/4/5$ for comparison. Similarly, all the results are averaged over 1000 trials. Specifically, in OFDMA system, the available bandwidth is equally divided into K REs and each UE communicates with the BS via one of the REs without any inter-user interference. Furthermore, in the SC-NOMA system, all the UEs communicate with the BS through the entire bandwidth; in the MC-NOMA system with SCMA scheme, the total bandwidth is equally divided into N REs and it allows sparse number of UEs to share the same RE; the MC-NOMA system with PDMA scheme is similar to that with SCMA scheme, but there is no constraint on the number of UEs that share the same RE. The QoS requirements for each UE are the same in different systems. As shown in Fig. 7, both SC-NOMA and MC-NOMA systems are more power-efficient than OFDMA system and the performance of the MC-NOMA systems are superior to that of the SC-MOMA system. Furthermore, an additional performance gain can be achieved in MC-NOMA system with PDMA scheme, comparing to that with SCMA technique. This is due to the fact that there is no limitation of sparsity in the PDMA scheme so that it is more likely for the UEs to select REs with better channel conditions to communicate with the BS. Hence, this validates and supports the superiority of our proposed scheme as well as the effectiveness of the developed deep learning-based approach.

V. Conclusions

The resource allocation problem for a downlink of SWIPT-enabled MC-NOMA system with PDMA scheme has been studied in this work. In particular, we focus on jointly optimizing characteristic pattern matrix, power allocation as well as TS ratio assignment for the total transmit power minimization problem with QoS requirements as well as the transmit power constraints. With the integer variable and the intra-band interference, the corresponding optimization problem is a non-convex and a mixed integer programming in its original form and thus it is extremely strenuous to determine the optimal solution. To resolve this problem, we have developed a deep learning-based approach which includes three phases, namely, data preparation, model training and solution running. Numerical results validate that our proposed approach can yield a solution which is similar to the ones derived by both exhaustive search method and genetic algorithm while significantly reduces the required computation time. Furthermore, it is also confirmed that the considered MC-NOMA with the application of PDMA outperforms MC-NOMA with SCMA, OFDMA and SC-NOMA in SWIPT-enabled systems in terms of the required minimum transmit power.

REFERENCES

[1] G. Chen, J. Tang, and J. P. Coon, "Optimal routing for multihop social-based D2D communications in the Internet of things," *IEEE Internet of Things Journal*, vol. 5, no. 3, pp. 1880–1889, Jun. 2018.

[2] P. Wang, J. Xiao, and L. P, "Comparison of orthogonal and non-orthogonal approaches to future wireless cellular systems," *IEEE Veh. Tech. Mag.*, vol. 1, no. 3, pp. 4–11, Sept. 2006.

[3] Z. Wei, J. Yuan, D. W. K. Ng, M. Elkashlan, and Z. Ding, "A Survey of Downlink Non-orthogonal Multiple Access for 5G Wireless Communication Networks," *[online].Available: https://arxiv.org/abs/1609.01856*, Sept. 2016.

[4] Y. Saito, A. Benjebbour, Y. Kishiyama, and T. Nakamura, "System-level performance of downlink non-orthogonal multiple access (NOMA) under various environments," in *Proc. IEEE 81st Vehicular Technology Conference (VTC Spring)*, May. 2015, pp. 1–5.

[5] F. Alavi, K. Cumanan, Z. Ding, and A. G. Burr, "Beamforming techniques for nonorthogonal multiple access in 5G cellular networks," *IEEE Trans. on Veh. Tech.*, vol. 67, no. 10, pp. 9474–9487, Oct. 2018.

[6] ——, "Robust beamforming techniques for non-orthogonal multiple access systems with bounded channel uncertainties," *IEEE Commun. Lett.*, vol. 21, no. 9, pp. 2033–2036, Sep. 2017.

[7] Z. Ding, X. Lei, G. K. Karagiannidis, R. Schober, J. Yuan, and V. K. Bhargava, "A survey on non-orthogonal multiple access for 5G networks: Research challenges and future trends," *IEEE Journal on Sel. Areas in Commun.*, vol. 35, no. 10, pp. 2181–2195, Oct. 2017.

[8] L. Dai, B. Wang, Y. Yuan, S. Han, C. I, and Z. Wang, "Non-orthogonal multiple access for 5G: solutions, challenges, opportunities, and future research trends," *IEEE Commun. Mag.*, vol. 53, no. 9, pp. 74–81, Sept. 2015.

[9] P. Xu and K. Cumanan, "Optimal power allocation scheme for non-orthogonal multiple access with α -fairness," *IEEE Journal on Sel. Areas in Commun.*, vol. 35, no. 10, pp. 2357–2369, Oct. 2017.

[10] H. Nikopour and H. Baligh, "Sparse code multiple access," in *Proc. IEEE 24th Annual International Symposium on Personal, Indoor, and Mobile Radio Communications (PIMRC)*, Sept. 2013, pp. 332–336.

[11] X. Dai, Z. Zhang, B. Bai, S. Chen, and S. Sun, "Pattern division multiple access: A new multiple access technology for 5G," *IEEE Wireless Commun.*, vol. 25, no. 2, pp. 54–60, Apr. 2018.

[12] Z. Wu, K. Lu, C. Jiang, and X. Shao, "Comprehensive study and comparison on 5G NOMA schemes," *IEEE Access*, vol. 6, pp. 18 511–18 519, 2018.

[13] X. Lu, P. Wang, D. Niyato, D. I. Kim, and Z. Han, "Wireless networks with RF energy harvesting: A contemporary survey," *IEEE Commun. Surveys Tuts.*, vol. 17, no. 2, pp. 757–789, Secondquarter 2015.

[14] L. R. Varshney, "Transporting information and energy simultaneously," in *2008 IEEE Int. Symp. Inf. Theory*, Jul. 2008, pp. 1612–1616.

[15] X. Zhou, R. Zhang, and C. K. Ho, "Wireless information and power transfer: Architecture design and rate-energy tradeoff," *IEEE Trans. on Commun.*, vol. 61, no. 11, pp. 4754–4767, Nov. 2013.

[16] D. W. K. Ng, E. S. Lo, and R. Schober, "Wireless information and power transfer: Energy efficiency optimization in OFDMA systems," *IEEE Trans. on Wireless Commun.*, vol. 12, no. 12, pp. 6352–6370, Dec. 2013.

[17] M. Zhang, K. Cumanan, L. Ni, H. Hu Alister G. Burr, and Z. Ding, "Robust beamforming for AN aided MISO SWIPT system with unknown eavesdroppers and non-linear EH model," in *Proc. IEEE Globecom Workshop*, Dec. 2018.

[18] M. Zhang, K. Cumanan, and A. Burr, "Secrecy rate maximization for miso multicasting SWIPT system with power splitting scheme," in *Proc. IEEE 17th International Workshop on Signal Processing Advances in Wireless Communications (SPAWC)*, Jul. 2016, pp. 1–5.

[19] J. Tang, D. K. C. So, N. Zhao, A. Shojaeifard, and K. Wong, "Energy efficiency optimization with SWIPT in MIMO broadcast channels for Internet of things," *IEEE Internet of Things Journal*, vol. 5, no. 4, pp. 2605–2619, Aug. 2018.

[20] S. Akbar, Y. Deng, A. Nallanathan, M. Elkashlan, and A. Aghvami, "Simultaneous wireless information and power transfer in k-tier heterogeneous cellular networks," *IEEE Trans. on Wireless Commun.*, vol. 15, no. 8, pp. 5804–5818, Aug. 2016.

[21] G. Chen, P. Xiao, J. R. Kelly, B. Li, and R. Tafazolli, "Full-duplex wireless-powered relay in two way cooperative networks," *IEEE Access*, vol. 5, pp. 1548–1558, 2017.

[22] Y. Xu, C. Shen, Z. Ding, X. Sun, S. Yan, G. Zhu, and Z. Zhong, "Joint beamforming and power-splitting control in downlink cooperative SWIPT NOMA systems," *IEEE Trans. on Sig. Process.*, vol. 65, no. 18, pp. 4874–4886, Sept. 2017.

[23] T. N. Do, D. B. da Costa, T. Q. Duong, and B. An, "Improving the performance of cell-edge users in MISO-NOMA systems using TAS and SWIPT-based cooperative transmissions," *IEEE Transactions on Green Communications and Networking*, vol. 2, no. 1, pp. 49–62, Mar. 2018.

[24] Z. Yang, Z. Ding, P. Fan, and N. Al-Dhahir, "The impact of power allocation on cooperative non-orthogonal multiple access networks with SWIPT," *IEEE Trans. on Wireless Commun.*, vol. 16, no. 7, pp. 4332–4343, Jul. 2017.

[25] N. T. Do, D. B. D. Costa, T. Q. Duong, and B. An, "A BNBF user selection scheme for NOMA-based cooperative relaying systems with SWIPT," *IEEE Commun. Lett.*, vol. 21, no. 3, pp. 664–667, Mar. 2017.

[26] J. Tang, T. Dai, M. Cui, X. Y. Zhang, A. Shojaeifard, K. Wong, and Z. Li, "Optimization for maximizing sum secrecy rate in SWIPT-enabled NOMA systems," *IEEE Access*, vol. 6, pp. 43 440–43 449, 2018.

[27] D. Zhai, M. Sheng, X. Wang, Y. Li, J. Song, and J. Li, "Rate and energy maximization in SCMA networks with wireless information and power transfer," *IEEE Commun. Lett.*, vol. 20, no. 2, pp. 360–363, Feb. 2016.

[28] J. Zeng, T. Lv, R. P. Liu, X. Su, M. Peng, C. Wang, and J. Mei, "Investigation on evolving single-carrier NOMA into multi-carrier NOMA in 5G," *IEEE Access*, vol. 6, pp. 48 268–48 288, 2018.

[29] B. Mao, Z. M. Fadlullah, F. Tang, N. Kato, O. Akashi, T. Inoue, and K. Mizutani, "Routing or computing? the paradigm shift towards intelligent computer network packet transmission based on deep learning," *IEEE Trans. on Comput.*, vol. 66, no. 11, pp. 1946–1960, Nov. 2017.

[30] P. Wang, S. Lin, and M. Luo, "A framework for qos-aware traffic classification using semi-supervised machine learning in SDNs," in *Proc. IEEE International Conference on Services Computing (SCC)*, Jun. 2016, pp. 760–765.

[31] L. Ghouti, "Mobility prediction using fully-complex extreme learning machines," in *22nd European Symposium on Artificial Neural Networks, Computational Intelligence and Machine Learning*, 2014, pp. 607 – 612.

[32] B. Bojovic, E. Meshkova, N. Baldo, J. Riihijrvi, and M. Petrova, "Machine learning-based dynamic frequency and bandwidth allocation in self-organized LTE dense small cell deployments," *EURASIP Journal on Wireless Communications and Networking*, vol. 2016, 12 2016.

[33] D. Tse and P. Viswanath, *Multiuser capacity and opportunistic communication*. Cambridge University Press, 2005, pp. 228–289.

[34] L. Lei, D. Yuan, C. K. Ho, and S. Sun, "Power and channel allocation for non-orthogonal multiple access in 5G systems: Tractability and computation," *IEEE Trans. on Wireless Commun.*, vol. 15, no. 12, pp. 8580–8594, Dec. 2016.

[35] G. E. Hinton, "Deep belief networks," *Scholarpedia*, vol. 4, no. 5, p. 5947, 2009, revision #91189.

[36] GreenTouch, *Mobile Communications WG architecture doc2: Refference scenarios*, May. 2013.